# EXPERIMENTAL INVESTIGATION OF THE PARTIALLY EVAPORATED ORGANIC RANKINE CYCLE FOR VARIOUS HEAT SOURCE CONDITIONS

Fabian Dawo[1]*, Jonathan Buhr[1], Christoph Wieland[1], Hartmut Spliethoff[1,2]

[1]Technical University of Munich, Institute for Energy Systems, Garching, Germany

[2] Bavarian Center for Applied Energy Research, Garching, Germany

*Corresponding Author: fabian.dawo@tum.de

## ABSTRACT

The Organic Rankine Cycle (ORC) could potentially play a vital role in the mitigation of climate change due to its ability to enable low-temperature heat sources for power generation. Next to the ORC, the partial evaporated Organic Rankine Cycle (PEORC) has recently received increased attention in the literature. In contrast to the ORC, the working fluid is not fully evaporated in the PEORC, which allows a higher utilization of the heat source due to a better match of the temperature profiles of heat source and working fluid during heat transfer. In this paper, both concepts are experimentally compared by their ability to generate net power outputs from a variety of different heat source conditions. Therefore, the heat source temperature is varied between 110 °C and 140 °C and the heat source mass flow is varied between 250 g/s and 400 g/s at a test rig. For all investigated heat source conditions, the optimal operating parameters, which provide the highest net system efficiencies, were identified. The results show that the PEORC outperforms the ORC for all investigated heat source conditions in terms of net system efficiency, especially at low heat source temperatures. While the thermal efficiency is higher in case of the ORC concept, the considerably higher heat transfer efficiency of the PEORC overcompensates the lower thermal efficiency.

## 1 INTRODUCTION

The energy sector can significantly contribute to the mitigation of climate change, especially due to the use of renewable and $CO_2$-neutral energy sources. In this context, the Organic Rankine Cycle (ORC) is a promising technology focusing on the reduction of energy induced $CO_2$ emissions by increasing the share of renewable energy sources for power and heat production. The ORC technology enables low-temperature heat sources for electric power generation and can, thus, be applied to industrial waste heat and renewable energy sources such as solar heat, geothermal brine or biomass combustion. Next to the ORC, the Trilateral-Flash-Cycle (TFC) is often discussed in the literature as a possible alternative low-temperature power generation cycle (Lai und Fischer 2012; Lecompte et al. 2015b). Smith et al. (Smith 1993) stated that the TFC can produce power outputs up to 80 % higher than Rankine cycles. In contrast to the ORC, the working fluid is not evaporated in the TFC and only heated to liquid saturation followed by a flash expansion in a two-phase expander. This way the temperature profiles of heat source and working fluid have a better match during heat exchange and thus exergy losses are reduced and the heat source can be exploited further. The partial evaporated Organic Rankine Cycle (PEORC) tries to combine the benefits of ORC and TFC and operates with a partially evaporated working fluid (Lecompte et al. 2013; Lecompte et al. 2015a). As expansion device twin-screw expanders are often suggested in the literature to be utilized as two-phase expanders (Read et al. 2014). According to (Smith et al. 2014) oil-flooded twin-screw expanders typically are more efficient compared to oil free (dry) expanders due to their lower clearances. Furthermore, oil-free twin-screw expanders are more expensive

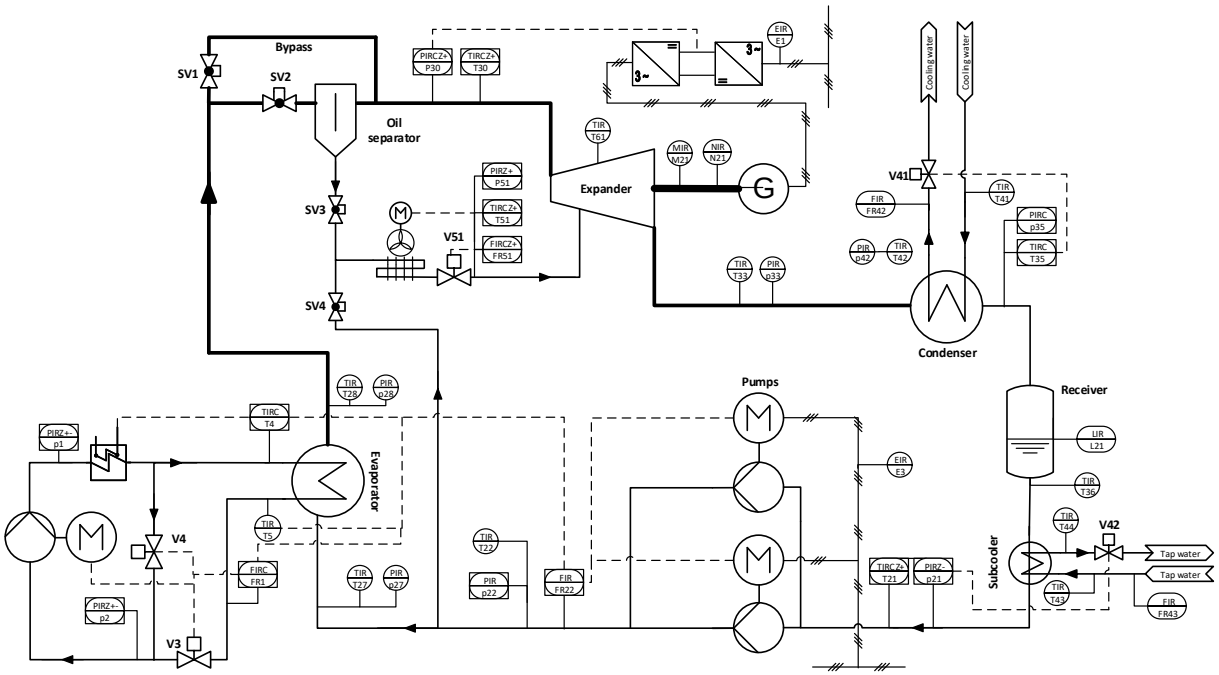


**Figure 1:** Simplified PID of the ORC test rig with control loops

and equipped with external timing gears, which prevent contact between the rotors. Even though the oil-flooded expander has some advantages, both twin-screw expander types should be suitable for two-phase expansion. However, the high fraction of liquid during expansion can potentially damage the expander rotors due to erosion.

While there are some theoretical studies on the PEORC and a variety of theoretical studies on the TFC in the literature, experimental studies are scarce. Therefore, to contribute to closing this research gap, this paper experimentally investigates the PEORC at an ORC test rig at various heat source conditions and compares its performance to the ORC. Therefore, temperature and mass flow were varied in an electrically heated hot water loop, which served as heat source. R1233zdE was employed as working fluid and a twin-screw compressor operated in reverse was utilized as expansion device. In order to allow a fair comparison of the ORC with the PEORC, the maximum net system efficiency of both concepts was determined for the same heat source conditions.

## 2 EXPERIMENTAL FACILITY AND METHODOLOGY

### 2.1 ORC test rig and control strategy

The experimental comparison is carried out with an existing ORC test rig. It was designed to study a variety of different ORC configurations and methods to optimize the ORC system performance such as combined heat and power architectures, two phase expansion or liquid injection to desuperheat the expander exhaust vapor. Figure 1 shows a simplified piping and instrumentation diagram (PID) of the test rig with all components and control loops relevant to this study. Therefore, the sensor labels are sometimes not in ascending order, as some sensors have been omitted for the sake of clarity.

The test rig consists of two main circuits: the actual ORC circuit and the heating circuit. The heating circuit is basically a hot water loop heated by a 200 kW electrical resistance heater. The electrical heater is controlled via pulse width modulation to maintain a constant heat source temperature at the evaporator inlet of up to 140 °C. A bypass control strategy is implemented to control the water mass flow through the evaporator (Alfa Laval CBH112-52H-F). For this purpose, a centrifugal heating circuit pump (Wilo IPn 40/160-2,2/2) is operated at constant rotational speed and the valves V3 and V4 are set such that the required water mass flow through the evaporator is achieved. This way mass flow and temperature of the heat source supplying the ORC can be controlled.

The circuit has two modes of operation, one for ORC operation with completely evaporated working fluid and one for PEORC operation with partially evaporated working fluid. These modes of operation mainly affect the handling of the lubricant oil in the circuit. The lubricant oil is circulated in the system together with the working fluid and ensures proper lubrication and cooling of the expander bearings. In ORC mode the lubricant oil is stripped from the fully evaporated working fluid in the oil separator (ESK Schulze BOS 2-54/42F) and then cooled down to 75 °C before being injected on the expander bearings. Therefore, the shut-off valves SV2 and SV3 are opened and the shut-off valves SV1 and SV4 are closed. The oil cooling is achieved by a controlled air-cooled heat exchanger by varying the rotational speed of the fan of the heat exchanger. Valve V51 is utilized to control the lubricant oil volume flow injected into the expander to the required value. Since the degree of separation in the oil separator is below unity a small amount of oil still enters the expander with the live vapor and lubricates the expander rotors. In case of PEORC operation, the oil separator cannot be used because the working fluid is not fully evaporated at any point of the cycle. Thus, there is always a quite large liquid fraction with a significant amount of liquid refrigerant, making it impossible to separate the oil from the refrigerant working fluid in the oil separator. Nevertheless, in order to ensure suitable cooling of the expander bearings, shut-off valve SV2 and SV3 are closed and shut-off valve SV4 and SV1 are opened during PEORC operation. This way cold liquid working fluid (extracted upstream of the evaporator) is injected onto the bearings providing proper cooling and the oil separator is bypassed which prevents flooding of the oil separator due to the high liquid fractions during PEORC operation.

The remaining part of the ORC circuit is not affected by the two investigated cycle concepts for the most part and the control strategy is almost the same as well. The fully evaporated and oil free live vapor or the partial evaporated working fluid enters the expander and is expanded to the condensation pressure level. The expander is an open-drive twin-screw compressor (Bitzer OSN5361-K) with a built in volume ratio of 5.6 operated in reverse. It is coupled to a generator, which converts the mechanical shaft power into electrical power. The electrical power is then fed to the grid after it passed a frequency converter. The frequency converter is furthermore used to control the rotational speed of the generator and expander respectively, which allows the control of the expander inlet pressure (corresponding to the evaporation pressure) of the system. The expanded vapor is subsequently desuperheated and fully condensed in a brazed plate heat exchanger (Alfa Laval CB112-170H). Therefore, the heat is transferred to a local cooling water grid and the condensation pressure is controlled by valve V41 by adjusting the cooling water mass flow. The 30 L receiver tank buffers the liquid working fluid and feeds it to the working fluid pumps. Before entering the pumps, the working fluid is slightly subcooled in another brazed plate heat exchanger (Alfa Laval CB60-60M-F) by tap water. The valve V42 controls the tap water flow to ensure the required net positive suction head (NPSH) for the working fluid pumps to prevent cavitation. The working fluid pumps are two positive displacement pumps (Verder G10 EKCEHFEMC), which are connected in parallel. The parallel configuration allows for a very wide range of possible working fluid mass flows because the system can be operated with only one or with both pumps at the same time. The pumps pressurize the working fluid and feed it to the evaporator to close the cycle. The rotational speed of the working fluid pumps is controlled to adjust the working fluid mass flow. In ORC operation the mass flow is controlled such that the required degree of superheating is obtained at the evaporator outlet. In case of the PEORC operation, the rotational speed of the pumps and the working fluid mass flow, respectively, is controlled to adjust the vapor quality at the evaporator outlet to the requested value. Since the vapor quality at the evaporator outlet cannot be measured in the current test rig design, the vapor quality of the working fluid is computed online. Therefore, the transferred heat in the evaporator is calculated by the following equation:

$$\dot{Q}_{HS} = \dot{m}_{HS}(h_4 - h_5) \tag{1}$$

The transferred heat is then used to determine the evaporator outlet enthalpy of the working fluid $h_{28}$.

$$h_{28} = h_{27} + \frac{\dot{Q}_{HS}}{\dot{m}_{ORC}} \tag{2}$$

Subsequently, the vapor quality is computed as a function of the evaporation pressure and the evaporator outlet enthalpy using REFPROP 10.0 (Lemmon et al. 2018). More details about the test rig and the

measurement uncertainties of all relevant sensors and the data acquisition system can be found in (Dawo et al. 2021a). The measurement uncertainty of the vapor quality calculated by Eq. (3) and (4) and the net system efficiency was determined by the Gaussian law of error propagation as described in (Eyerer et al. 2019). Using this method, results in a measurement uncertainty of the vapor quality of 1.7 to 34 %. The rarely occurring high measurement uncertainties of around 30 % occur at low values of the transferred heat and working fluid mass flows due to the constant part of the measurement uncertainties. The mean measurement uncertainty of the vapor quality for all operating points in PEORC mode is 8 %. The measurement uncertainty of the net system efficiency ranges from 0.007 to 0.3 % and has a mean value of 0.16 % for all operating points in PEORC mode.

### 2.2 Experimental methodology

The refrigerant R1233zdE, which is a low-GWP alternative to the state of the art working fluid in ORC applications R245fa (Dawo et al. 2021b), was utilized in all experiments. It is mixed with approximately 5 mass% lubricant oil (Reniso Triton SE 220), which is circulated in the cycle together with the refrigerant forming a working fluid mixture. In total 261 stationary operating points were investigated for this study. 87 in ORC conditions with fully evaporated working fluid and 174 in PEORC conditions with varying live vapor qualities. For all operating points, stationary conditions were maintained for at least 10 min with fixed controller setpoints. In order to detect the time span with the highest stationarity an algorithm, described in detail in (Eyerer et al. 2020), was used. To ensure the reproducibility of the experiments, a reference point was evaluated in each measurement series and compared with all previous measurement series for ORC and PEORC operation. This way any damage or changes to/in the experimental system would become evident during the experimental campaign.

A wide variety of different heat source conditions was investigated to compare the performance of the ORC and the PEORC. The heat source temperature was varied between 110 °C and 140 °C in steps of 10 K and the heat source mass flow was varied between 250 g/s and 350 g/s in steps of 50 g/s. For a heat source temperature of 120 °C, additionally a heat source mass flow of 400 g/s was investigated. This gives in total 13 different heat source conditions. The condensation temperature was fixed to 40 °C for all measurements. For all these heat source conditions, the maximum net system efficiency was determined for ORC and PEORC. Therefore, in case of the PEORC evaporation pressure and live vapor quality were varied to find the optimal combination. In case of the ORC the degree of superheating was fixed at 10 K and only the live vapor pressure was varied. The heat source temperature and mass flow combination of 120 °C and 350 g/s was chosen as a reference heat source and therefore was experimentally investigated in more detail. For the remaining heat source conditions, the focus was on identifying the optimal operating parameters. In order to correctly describe the zeotropic behavior of the oil-refrigerant mixture, the model introduced in (Dawo et al. 2021b) was used in all calculations. This model is based on Raoult's law and allows the computation of the liquid phase composition of the refrigerant-oil mixture as a function of temperature, pressure and total oil mass fraction. For the vapor phase, it is assumed that only refrigerant is present due to the significantly higher evaporation temperature of the oil. In order to use the model, the total mass fraction of the lubricant oil in the mixture and a fitting parameter specific to the oil-refrigerant combination has to be known.

## 3 RESULTS AND DISCUSSION

### 3.1 Reference heat source

The aim of this paper is to experimentally compare the performance of the PEORC with the ORC at various heat source conditions. Therefore, in case of the ORC evaporation pressure and degree of superheating and in case of the PEORC evaporation pressure and live vapor quality were varied to identify the optimal operating parameters. The optimal operating parameters are defined by the maximum net system efficiency in this paper. The net system efficiency is defined by the ratio of the net power output of the system and the maximum capacity of the heat source related to a reference state.

$$\eta_{sys,net} = \frac{P_{el,gross} - P_{el,pump}}{\dot{m}_{HS} \cdot \left(h_{HS,in} - h_{HS,ref}\right)} \quad (5)$$

The reference temperature to determine the reference enthalpy of the heat source is 40 °C, which equals the condensation temperature. The net power output of the system is defined by the gross power fed to the grid minus the power consumption of the working fluid pumps. The net system efficiency thus describes how well a system exploits a given heat source.

To better understand the process to identify the optimal operational parameters for the given heat source conditions, **Figure 2** shows the system efficiency for ORC and PEORC for the reference heat source (120 °C and 350 g/s) as a function of the evaporation pressure and degree of superheating and the evaporation pressure and live vapor quality, respectively. The black dots represent the experimentally measured data points and the contour plot is a polynomial fit to them. Both contour plots share a common color bar for the system efficiency and the maximum net system efficiency is marked with red diamond shaped markers. As can be seen in **Figure 2** a) the maximum net system efficiency can be found at an intermediate evaporation pressure and the degree of superheating only has minor impact on the net system efficiency of the ORC. Since a refrigerant-lubricant mixture is utilized as working fluid in the ORC, at small degrees of superheating a considerable amount of refrigerant is still dissolved in liquid form in the lubricant oil and is not evaporated yet, due to the zeotropic nature and non-isothermal evaporation of these kind of mixtures (Dawo et al. 2021b). Therefore, to make sure that the working fluid is at least almost fully evaporated the degree of superheating was fixed to 10 K for all other heat source conditions and only the evaporation pressure was varied. In case of the PEORC the live vapor quality and the evaporation pressure have a significant impact on the net system efficiency as can be seen in **Figure 2** b). The maximum is again located at intermediate evaporation pressure levels and is quite similar to the ORC case. However, for the PEORC the vapor quality has a significant impact on the net system efficiency. With decreasing vapor qualities, the efficiency first increases up to a vapor quality of about 0.3 and then sharply drops with further decreasing vapor qualities forming a clear optimum. Therefore, in case of the PEORC both parameters were varied in the experimental campaign to identify the optimal combination for all heat source conditions.

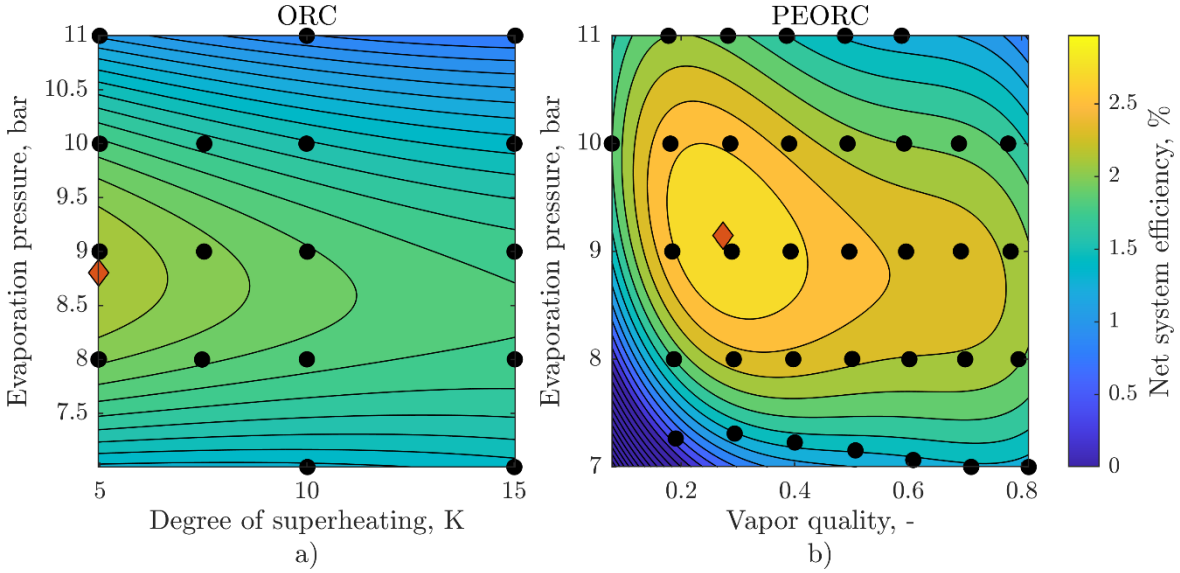


**Figure 2:** Polynomial fit of the net system efficiency of ORC a) and PEORC b) as a function of evaporation pressure and degree of superheating in case of the ORC and evaporation pressure and vapor quality in case of the PEORC. The maxima in net system efficiency are marked with the red diamond shape markers.

### 3.2 Comparison for various heat source conditions

The procedure explained in the last section was repeated for all investigated heat source conditions and the maximum net system efficiency was determined by a polynomial fit to the experimental data. These optimal efficiencies are illustrated in **Figure 3** for ORC and PEORC by contour plots. The black markers illustrate the experimentally investigated heat source conditions and the contour plot in between is interpolated from these data points. Thus, **Figure 3** shows the maximum possible net system efficiency for ORC and PEORC for every heat source temperature and mass flow combination. For the sake of comparability, both contour plots share one common color bar. In both cases the net system efficiency is mainly a function of the heat source temperature and almost independent of the heat source mass flow. That was kind of to be expected, since the mass flow only scales the available heat but does not change the exergy level and thus the cycle efficiency is unaffected apart from part-load effects even though the power output obviously increases with increasing heat source mass flow. The heat source temperature on the other hand has a significant impact on the net system efficiency, which increases approximately linear with increasing heat source temperatures for ORC and PEORC, due to the higher exergy level of the heat source. Furthermore, the figure shows that the PEORC outperforms the ORC for all investigated heat source conditions. At low heat source temperatures, the PEORC achieves up to 80 % higher net system efficiencies compared to the ORC. This massive advantage drops to about 20 % higher net system efficiencies by the PEORC at heat source temperatures of 140 °C. The optimized operating parameters (evaporation pressure and vapor quality) for ORC and PEORC are summarized in Table 1. The values show that for a low heat source temperature the optimal evaporation pressure of ORC and PEORC does not differ much. For higher heat source temperatures the PEORC should be operated at higher evaporation pressures compared to the ORC. The optimal vapor quality in case of the PEORC also increases with rising heat source temperatures. To further explain and detail these differences in the maximum net system efficiency of ORC and PEORC, **Figure 4** shows the thermal efficiency and the heat transfer efficiency for ORC and PEORC at the operating conditions corresponding to the maximum net system efficiency (cf. **Figure 3**). The thermal efficiency and the heat transfer efficiency are defined by:

$$\eta_{th,net} = \frac{P_{el,gross} - P_{el,pump}}{\dot{m}_{ORC} \cdot (h_{28} - h_{27})} \tag{6}$$

$$\eta_{ht} = \frac{\dot{m}_{ORC} \cdot (h_{28} - h_{27})}{\dot{m}_{HS} \cdot (h_{HS,in} - h_{HS,ref})} \tag{7}$$

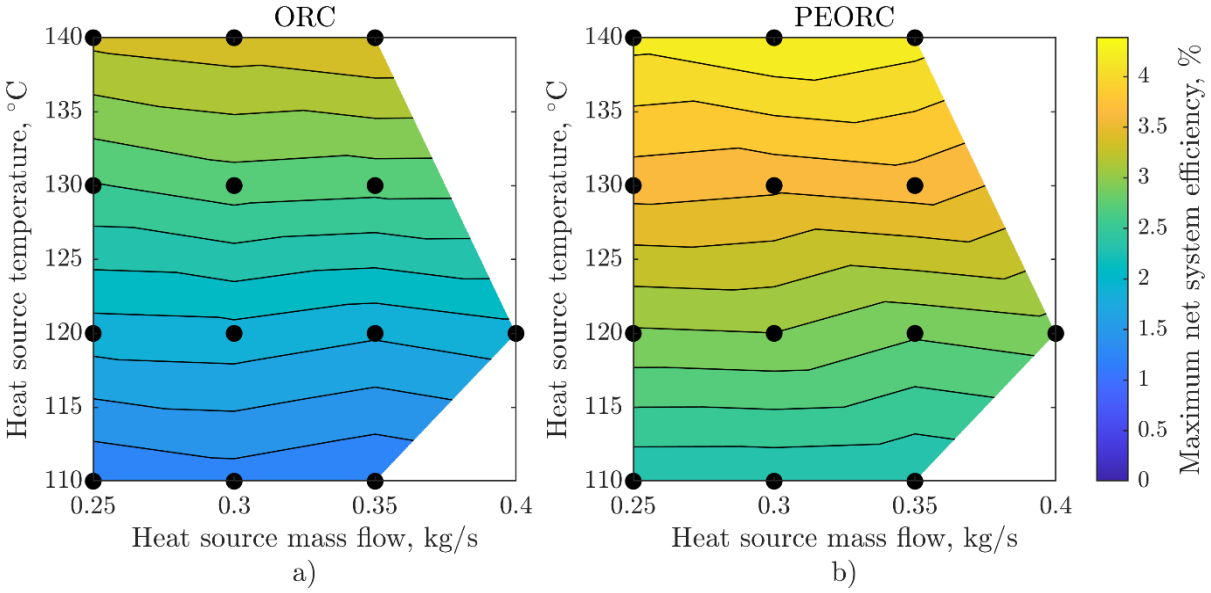


**Figure 3:** Maximum net system efficiencies of ORC a) and PEORC b) for various heat source temperatures and mass flows

**Table 1:** Optimal operating parameters for ORC and PEORC for all investigated heat source conditions

| **Heat source** | | **ORC** | **PEORC** | |
|---|---|---|---|---|
| Temperature, °C | Mass flow, g/s | Evaporation pressure, bar | Evaporation pressure, bar | Vapor quality, - |
| 110 | 250 | 7.41 | 7.66 | 0.21 |
| 110 | 300 | 7.70 | 7.97 | 0.20 |
| 110 | 350 | 7.81 | 8.24 | 0.22 |
| 120 | 250 | 8.23 | 8.60 | 0.25 |
| 120 | 300 | 8.44 | 9.06 | 0.26 |
| 120 | 350 | 8.73 | 9.03 | 0.33 |
| 120 | 400 | 8.64 | 9.22 | 0.28 |
| 130 | 250 | 8.55 | 9.32 | 0.34 |
| 130 | 300 | 8.93 | 9.67 | 0.32 |
| 130 | 350 | 8.96 | 9.58 | 0.35 |
| 140 | 250 | 9.34 | 10.17 | 0.39 |
| 140 | 300 | 9.84 | 10.32 | 0.40 |
| 140 | 350 | 9.76 | 11.03 | 0.40 |

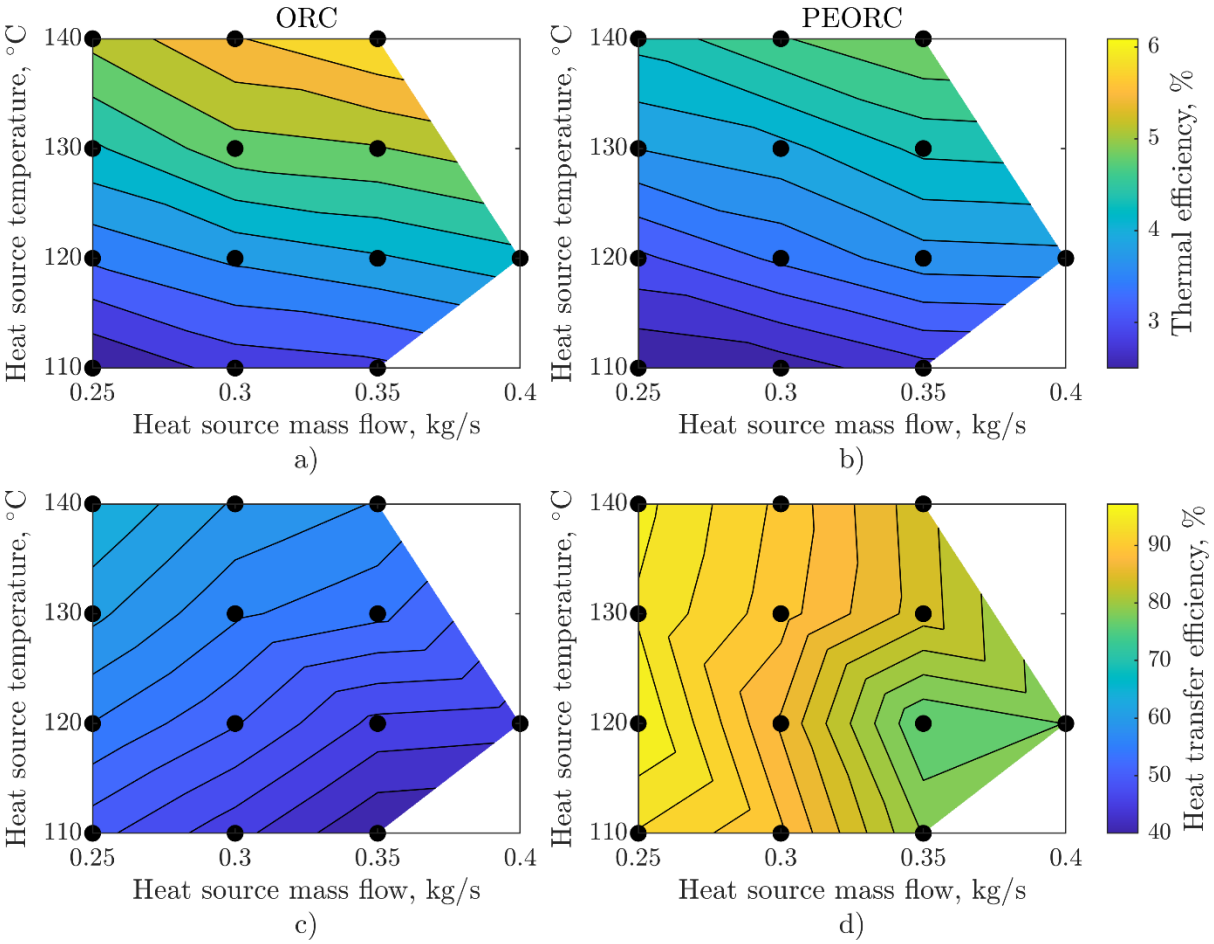


**Figure 4:** Thermal efficiency (a) and b)) and heat transfer efficiency (c) and d)) as a function of heat transfer temperature and mass flow for ORC (a) and c)) and PEORC (b) and d)) at maximum net system efficiency

While the thermal efficiency describes how well the process transforms the heat supplied to it into power, the heat transfer efficiency describes how well the process is able to exploit the heat source. The net system efficiency (cf. Eq.(5)) is the product of the thermal efficiency (Eq. (8)) and the heat transfer efficiency (Eq. (9)). As can be seen in **Figure 4** the thermal efficiency of the ORC and PEORC is fairly low, due to the low temperature level of the heat source. Nonetheless, the thermal efficiency is higher for the ORC compared to the PEORC. This is a result of the higher enthalpy and temperature level the ORC is operating on and thus the higher exergy level at the evaporator outlet. For the same reason, the thermal efficiency increases with increasing heat source temperatures for both cycle concepts. In case of the heat transfer efficiency, on the other hand the main advantage of the PEORC becomes evident. Due to the partial evaporation of the working fluid, the pinch-point limitation in the evaporator is less limiting for the PEORC than for the ORC and the heat source can be exploited to a greater extent. This leads to significantly higher heat transfer efficiencies in case of the PEORC, which overcompensate the lower thermal efficiencies and therefore lead to higher system efficiencies. Furthermore, the heat transfer efficiency drops with increasing heat source mass flow due to the fixed heat transfer surface of the evaporator.

## 4 CONCLUSION

In this paper, the partial evaporated Organic Rankine Cycle (PEORC) is experimentally investigated and compared to the ORC for various heat source conditions. Therefore, an ORC test rig was slightly modified to enable the PEORC operation. R1233zdE was chosen as the working fluid and was mixed with approximately 5 mass% lubricant oil. Both concepts were investigated for a heat source temperature range of 110 °C to 140 °C and a heat source mass flow range of 0.25 kg/s to 0.4 kg/s. The maximum net system efficiency for ORC and PEORC was experimentally determined for all heat source conditions and chosen as a benchmark to compare the two cycle concepts. To identify the maximum system efficiency, the evaporation pressure was varied at a fixed degree of superheating of 10 K in case of the ORC and the evaporation pressure and the live vapor quality were varied in case of the PEORC. Based on the analysis of the experimental data, the following conclusions can be drawn:

- The net system efficiency of the PEORC is up to 80 % higher at low heat source temperatures.
- The ORC concept shows higher thermal efficiencies due to its higher temperature and exergy level.
- The PEORC has much higher heat transfer efficiencies compared to the ORC and is therefore able to exploit the heat source to a greater extent.

Further experimental investigations will focus on the impact of the two-phase expansion on the twin-screw expander and the modeling of the two-phase expansion.

## ACKNOWLEDGEMENT

Funding from the Bavarian State Ministry of Education, Science and the Arts in the framework of the project Geothermal-Alliance Bavaria is gratefully acknowledged.

## NOMENCLATURE

| | | |
|---|---|---|
| h | Specific enthalpy | J/kg |
| $\dot{m}$ | Mass flow | kW |
| P | Power | kW |
| $\dot{Q}$ | Heat flow | kW |
| $\eta$ | Efficiency | - |

**Subscript**

| | |
|---|---|
| el | Electrical |
| HS | Heat source |
| ht | Heat transfer |
| ORC | Organic Rankine Cycle |
| ref | Reference |
| th | Thermal |

## REFERENCES

Dawo, Fabian; Eyerer, Sebastian; Pili, Roberto; Wieland, Christoph; Spliethoff, Hartmut (2021a): Experimental investigation, model validation and application of twin-screw expanders with different built-in volume ratios. In: *Applied Energy* 282 (3), S. 116139. DOI: 10.1016/j.apenergy.2020.116139.

Dawo, Fabian; Fleischmann, Jonas; Kaufmann, Florian; Schifflechner, Christopher; Eyerer, Sebastian; Wieland, Christoph; Spliethoff, Hartmut (2021b): R1224yd(Z), R1233zd(E) and R1336mzz(Z) as replacements for R245fa. Experimental performance, interaction with lubricants and environmental impact. In: *Applied Energy* 288 (1), S. 116661. DOI: 10.1016/j.apenergy.2021.116661.

Eyerer, Sebastian; Dawo, Fabian; Kaindl, Johannes; Wieland, Christoph; Spliethoff, Hartmut (2019): Experimental investigation of modern ORC working fluids R1224yd(Z) and R1233zd(E) as replacements for R245fa. In: *Applied Energy* 240, S. 946–963. DOI: 10.1016/j.apenergy.2019.02.086.

Eyerer, Sebastian; Dawo, Fabian; Pili, Roberto; Schifflechner, Christopher; Wieland, Christoph; Spliethoff, Hartmut (2020): Experimental and numerical investigation of an advanced injection cooling concept for Organic Rankine Cycles. In: *Energy Conversion and Management* 224 (10), S. 113342. DOI: 10.1016/j.enconman.2020.113342.

Lai, Ngoc Anh; Fischer, Johann (2012): Efficiencies of power flash cycles. In: *Energy* 44 (1), S. 1017–1027. DOI: 10.1016/j.energy.2012.04.046.

Lecompte, S.; Huisseune, H.; van den Broek, M.; Paepe, M. de (2015a): Methodical thermodynamic analysis and regression models of organic Rankine cycle architectures for waste heat recovery. In: *Energy* 87 (8), S. 60–76. DOI: 10.1016/j.energy.2015.04.094.

Lecompte, Steven; Huisseune, Henk; van den Broek, Martijn; Vanslambrouck, Bruno; Paepe, Michel de (2015b): Review of organic Rankine cycle (ORC) architectures for waste heat recovery. In: *Renewable and Sustainable Energy Reviews* 47, S. 448–461. DOI: 10.1016/j.rser.2015.03.089.

Lecompte, Steven; van den Broek, M.; Paepe, M. de (2013): Thermodynamic analysis of the partially evaporating trilateral cycle. 2nd International Seminar on ORC Power Systems, Rotterdam, Netherlands, October, 2013.

Lemmon, E. W.; Bell, I. H.; Huber, M. L.; McLinden, M.O (2018): NIST Standard Reference Database 23: Reference Fluid Thermodynamic and Transport Properties-REFPROP, Version 10.0, National Institute of Standards and Technology. Standard Reference Data Program. Gaithersburg, 2018.

Read, Matthew; Stosic, Nikola; Smith, Ian K. (2014): Optimization of Screw Expanders for Power Recovery From Low-Grade Heat Sources. In: *Energy Technology & Policy* 1 (1), S. 131–142. DOI: 10.1080/23317000.2014.969454.

Smith, I. K. (1993): Development of the Trilateral Flash Cycle System. Part 1: Fundamental Considerations. In: *Proceedings of the Institution of Mechanical Engineers, Part A: Journal of Power and Energy* 207 (3), S. 179–194. DOI: 10.1243/PIME_PROC_1993_207_032_02.

Smith, Ian K.; Stosic, Nikola; Kovacevic, Ahmed (2014): Power recovery from low grade heat by means of screw expanders. [Second edition]. Cambridge, UK, Burlington: Woodhead Publishing; Elsevier Science (Woodhead Publishing in mechanical engineering). Online verfügbar unter http://www.sciencedirect.com/science/book/978-1-78242-189-4.